0270-6474/81/0109-0981$02.00/0

The Journal of Neuroscience
Vol. 1, No. 9, pp. 981-992
September 1981

THE VISUAL CLAUSTRUM OF THE CAT

II. The Visual Field Map[1]

SIMON LEVAY AND HELEN SHERK

Department of Neurobiology, Harvard Medical School, Boston, Massachusetts 02115

Abstract

Physiological and anatomical methods were used to study the representation of the visual field in the cat's dorsocaudal claustrum. In one set of experiments, the visual receptive fields of claustral neurons were plotted in multiple electrode penetrations. In another set of experiments, the termination of the corticoclaustral pathway was examined autoradiographically after the injection of [^{3}H]proline at retinotopically defined sites in the visual cortex.

Results obtained by the two methods were in close agreement. The claustrum was found to contain a single, orderly map of the contralateral hemifield and a small part of the ipsilateral field. High elevations are represented caudally and ventrally, low elevations rostrally and dorsally. The surface of the claustrum represents the periphery of the visual field, while the vertical meridian lies more ventrally, where the visual claustrum abuts the non-visual part of the nucleus. Visual field lines (isoazimuths or isoelevations) are represented as planes in the claustrum. The map is unusual in that isoazimuth planes are strongly curved and nested within each other, with peripheral ones enclosing those closer to the vertical meridian. This arrangement permits an expanded representation of the periphery compared with what is seen in visual cortex.

The inputs from areas 17, 18, 19, 21a, and PMLS (posteromedial lateral suprasylvian area) are convergent, each projecting retinotopically to the entirety of the claustral map.

The first paper in this series (LeVay and Sherk, 1981) defined a dorsocaudal zone within the cat's claustrum that is connected reciprocally with the visual cortex but that has few connections with non-visual regions of the brain. In the present study, we ask whether the claustrum, like most purely visual structures, possesses a map of the visual field, and if so, how the map is laid out within the small and curiously shaped space available to it.

Two complementary techniques were used to approach this question. The first was physiological mapping: receptive fields were plotted on closely spaced vertical penetrations. The second involved autoradiography: we injected radioactive tracers at physiologically defined sites within several of the visual cortical maps and examined the position and shape of the resulting terminal labeling in the claustrum. By direct physiological mapping, it is possible to delineate the general layout of the map within the claustrum and also, on a finer scale, to examine its degree of orderliness. Given the highly distorted map that turns out to exist in the claustrum, however, it would be difficult to define the entire representation of a single visual field point physiologically. It is exactly this information that is provided by an autoradiographic experiment. The autoradiographic approach can also tell us whether the projections from the individual cortical areas converge onto a common map in the claustrum or whether each cortical area projects to a separate zone.

Earlier work in this area has led to conflicting conclusions. While Jayaraman and Updyke (1979) and Squatrito et al. (1980a) have concluded that no topographic organization exists in the cat's claustrum, Carey et al. (1980) did find evidence suggestive of retinotopic order in the tree shrew. In a study concurrent with our own, Olson and Graybiel (1980) have described the general layout of a visual field map in the cat's claustrum. Our findings are in agreement with their results. The present study shows that the claustral map is highly distorted in three-dimensional space and favors the representation of the peripheral field.

Materials and Methods

The cats used for anatomical mapping are listed in Table I. The techniques used for physiological recording, injection of tracers, histology, and autoradiography were described in the previous paper (LeVay and Sherk, 1981).

[1] We wish to thank R. Leibowitz for histology, M. Peloquin for photography, and T. Wiesel, C. Gilbert, and P. Desan for comments on the manuscript. This work was supported by National Institutes of Health Grant EY-R01-1960.

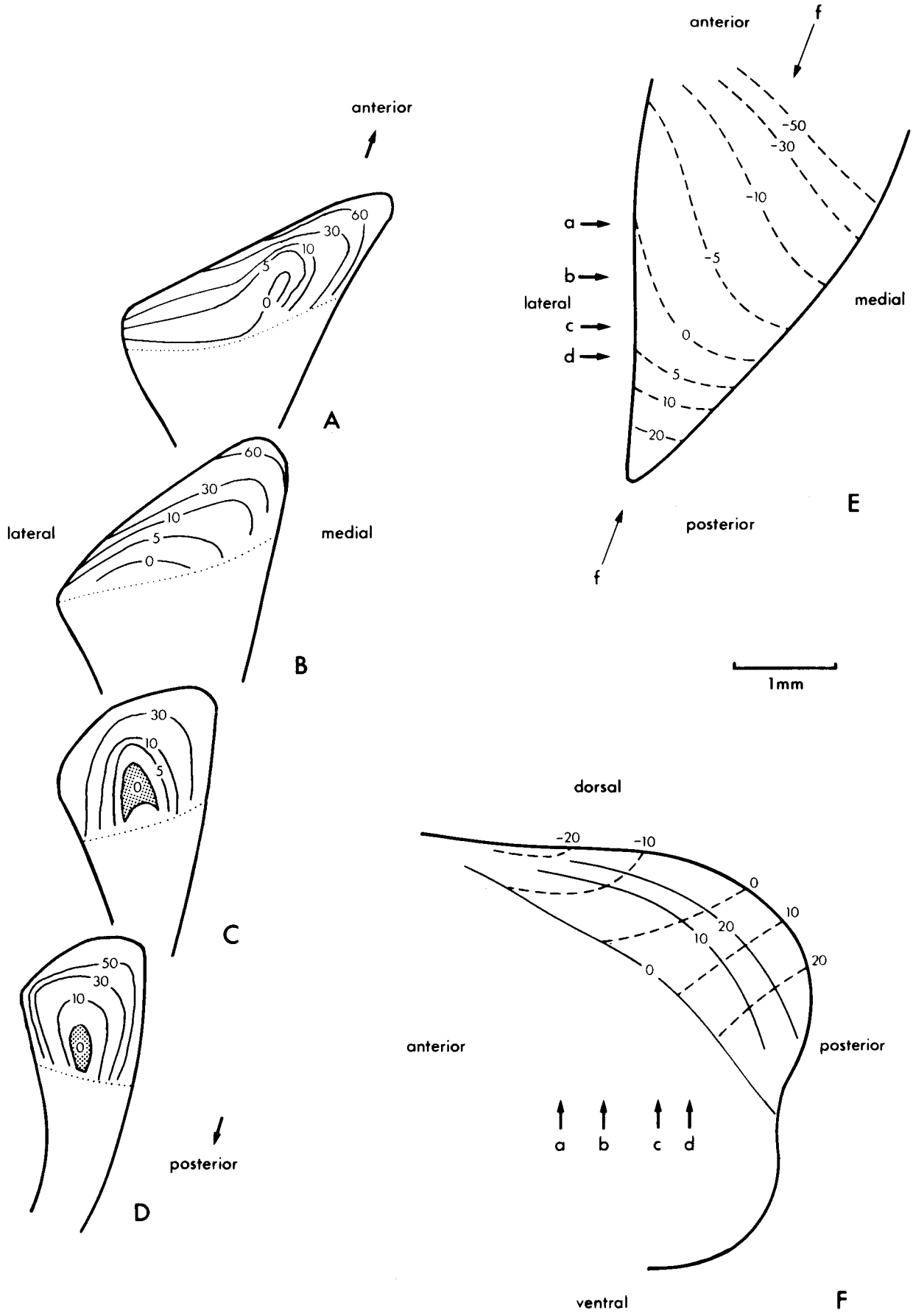
anterior
60
30
10
5
0
A
lateral
medial
60
30
10
5
0
B
30
10
5
0
C
50
30
10
0
posterior
D
anterior
f
-50
-30
-10
-5
a
b
lateral
c
d
0
5
10
20
medial
posterior
f
E
1mm
dorsal
-20
-10
0
10
20
10
20
0
anterior
posterior
a
b
c
d
ventral
F

Usually, a single injection (commonly 0.1 μl of [^{3}H]proline at a concentration of 50 μCi/μl) was made in each animal. In most cases (18 injections), the cortical area being injected and the retinotopic locus of the injection site within that area were identified by physiological mapping prior to the injection and by recording through the injection micropipette itself. An additional three injections were made into area 17, and one into the posteromedial lateral suprasylvian area (PMLS), without recording; in these cases, we estimated the corresponding visual field positions by locating the labeled corticogeniculate projection zone within the geniculate visual field map (Sanderson, 1971; see Table I).

In one cat (No. 474), [^{3}H]proline and [^{14}C]proline were injected at different visual field positions in area 17. One injection consisted of 0.1 μl of L-[2,3-^{3}H]proline (specific activity, 20 to 40 Ci/mmol) at a concentration of 50 μCi/μl (giving an injection of 5 μCi) and the other was of 0.1 μl of uniformly labeled L-[^{14}C]proline (specific activity, 250 mCi/mmol) at a concentration of 2.5 μCi/μl (giving an injection of 0.25 μCi). The two cortical injection sites and the two projection zones within the claustrum appeared about equally densely labeled when processed by our usual autoradiographic methods (dipping in Kodak NTB2 emulsion). The two isotopes were distinguished by mounting adjacent sections on slides and pressing them against x-ray film, whose protective coating greatly attenuates the β emissions from tritium relative to those from ^{14}C. After 2 weeks' exposure, the x-ray film was developed in D19.

Another compound, ^{125}I-wheat germ agglutinin (^{125}I-WGA), though intended for use as a retrograde tracer, also gave strong anterograde labeling and hence was useful in the mapping of corticoclaustral projections. The anterogradely transported label was evident as silver grains densely filling the neuropil between cells.

In the physiological mapping experiments, we have considered isoazimuths and isoelevations to be parallel to the vertical and horizontal meridians, respectively, at all eccentricities and have also corrected the distortion in the distances measured on the tangent screen so that the values are equivalent to ones measured on a hemisphere 145 cm from the cat.

Results

Physiological mapping

Both the physiological and anatomical results demonstrated that the claustrum contains a single, orderly representation of the contralateral hemifield. We will first present a summary diagram of this representation, based on physiological mapping, and then discuss in detail the findings from which we reconstructed the visual field map. Figure 1 shows three different views of the map: a set of coronal sections (*A* to *D*), a dorsal view (*E*), and a section cut along the long axis of the claustrum (i.e., with the anterior end rotated slightly inward from the parasagittal plane) (*F*).

The entire visual field representation can be seen on a single longitudinal section, such as that of Figure 1*F*. Peripheral azimuths are dorsal in the nucleus, and the vertical meridian is ventral. The horizontal meridian cuts across the map diagonally, with lower visual fields lying anterior and above the meridian and upper fields lying posterior and below it.

The claustral map is actually more complex than the diagram of Figure 1*F* suggests. In part, this complexity stems from the fact that the visual claustrum is a three-dimensional structure so that points in the visual field are represented in the claustrum by lines and visual field lines by planes. Thus, in a set of coronal sections (Fig. 1, *A* to *D*), it is apparent that isoazimuth lines are represented by a series of curved sheets. Isoelevation lines are likewise represented by a series of planes. These are rotated, lateral edge forward, from the coronal plane (Fig. 1*E*) and also are tilted backward (Fig. 1*F*). The shape of the claustrum changes markedly as one progresses from the caudal pole forward. Since the layout of isoazimuth sheets reflects the shape of the claustral outline, they are strongly curved caudally (Fig. 1, *C* and *D*) but tend to be flat, bending down only on the medial side further rostrally (Fig. 1, *A* and *B*).

The summary diagrams of Figure 1 are based on results obtained from five cats. In three of these, both the length and breadth of the visual region were explored, while in the other two, detailed mapping was done in a single coronal plane. In each animal, 6 to 19 vertical electrode penetrations were made through the claustrum; receptive fields were plotted along each penetration at 50- or 100-μm intervals, giving a total of 374 recording sites.

Three such penetrations from one experiment (Fig. 2) illustrate the general layout of the map. These show the receptive field progressions obtained at three different anteroposterior levels, each penetration passing approximately through the middle of the mediolateral extent of the nucleus. On each penetration, the first cells encountered at the dorsal margin of the claustrum had receptive fields in the far periphery of the visual field. As the electrode descended through the claustrum, receptive fields of successive units moved in an orderly sequence toward the vertical meridian. The sequence either ended at the meridian (*penetrations 2* and *3*) or continued a

Figure 1. Summary diagram of the receptive field map in the left claustrum. *Parts A* to *D* are coronal sections, showing the isoazimuths (*solid lines*) and the lower limit of the visual area (*dotted line*). Where the latter is displaced ventrally from the 0° isoazimuth (vertical meridian), a small representation of part of the ipsilateral hemifield was found, but the location of this zone was inconstant. Note that, in the more caudal sections (*C* and *D*), the vertical meridian forms a central core (*shaded area*), while more anteriorly, it is flattened. *Part E* is a dorsal view of the caudal claustrum, showing the layout of the isoelevations (*dashed lines*). These are drawn not as they meet the dorsal surface of the claustrum but at a level halfway through the dorsoventral extent of the visual region. The levels of the sections illustrated in *parts A* to *D* are shown also (*a* to *d*). *Part F* is a view of the entire visual field map as seen in a vertical section cut along the long axis of the claustrum (i.e., rotated about 25° from the parasagittal plane, front inward, as indicated by the letter *f* in *Part E*).

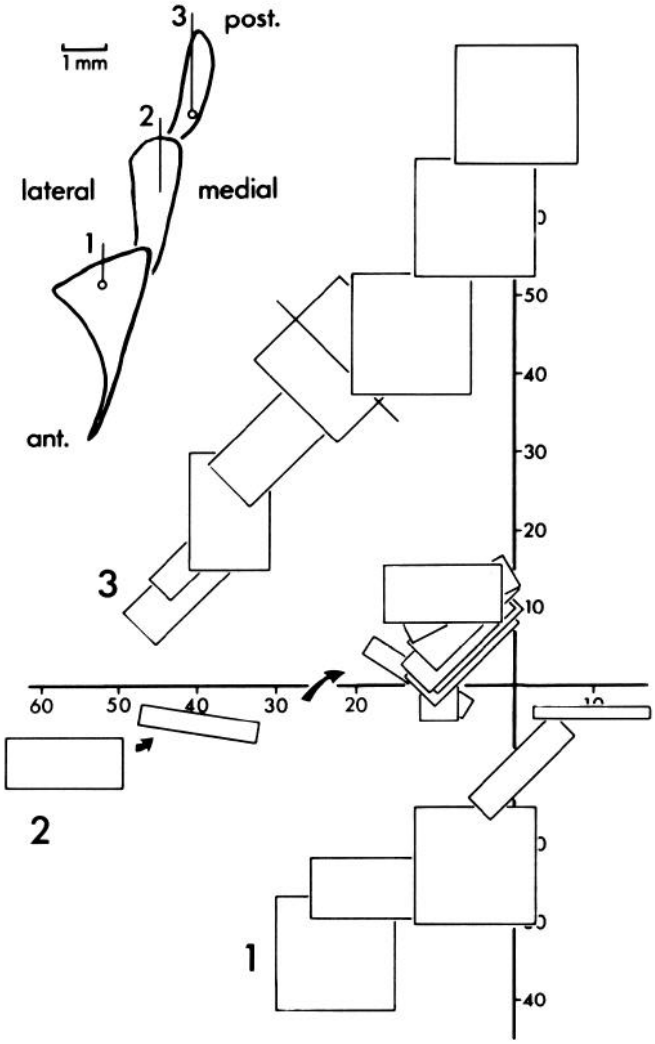

Figure 2. Receptive fields plotted on three vertical penetrations into the right claustrum of a single cat at different anteroposterior levels: *1* is the most anterior (near the rostral limit of the visual region), and *3* is near the caudal pole. *Tracks 1* and *3* terminate with lesions as shown by *circles* in the *inset drawings* (see also Fig. 3). For each penetration, successive receptive fields are shown as overlapping those recorded earlier. Thus, the progression is toward the vertical meridian and upward for all three penetrations, but at different elevations in the visual field depending on the anteroposterior level of the penetration. Where there are gaps (*penetration 2*), the sequence of receptive fields is shown by *arrows*. Fields were plotted at 100-μm intervals, but, for clarity, in *penetration 3*, only every other field is drawn. For cells having a preferred orientation, this is shown by the orientation of the long axis (length) of the field or (for one cell) by the orientation of a *line bisecting the field*. The width of each receptive field was plotted by hand, but the length has been drawn arbitrarily as 15°. This was done because, as discussed in the following paper (Sherk and LeVay, 1981), the exact limits of these elongated fields were difficult to plot with hand-held stimuli. For cells whose orientation preference was not established, the fields are shown as *15° squares*. Closer study might well have shown these cells to be orientation selective also. *ant.*, anterior; *post.*, posterior.

short distance into the ipsilateral visual hemifield (*penetration 1*). As well as moving in toward the vertical meridian, fields also moved upward as the electrode descended. A similar inward and upward movement of receptive fields was seen in nearly every penetration that we made in the claustrum.

What distinguished the three receptive field progressions of Figure 2 from one another was the elevation at which each occurred: the most caudal pass (*3*) gave receptive fields that crossed the upper quadrant of the visual field, the middle one (*2*) gave a progression roughly at the level of the horizontal meridian, while the most anterior one (*1*) gave a progression across the lower quadrant. Thus, a series of penetrations in a rostrocaudal sequence spans the entire visual hemifield.

The distance traveled by the electrode through the claustrum before visual responses ceased was not the same on all three penetrations. It was greatest at the caudal end (*penetration 3*, about 2.2 mm, see Fig. 3) and least anteriorly (*penetration 1*, about 0.7 mm). In each case, the point where visual responses ceased was within the claustrum itself, rather than at an edge. This confirms our conclusion, based on anatomical evidence, that there is a non-visual region of the claustrum below the visual area (LeVay and Sherk, 1981). This is the zone that we have shown to be connected with the splenial (cingulate) gyrus of the cerebral cortex and thus have called limbic claustrum. Curiously, responses did not cease abruptly at the visual-limbic border. Rather, cells near the border gave gradually weaker and more erratic responses, and often visual responses were obscured by a higher and more bursty spontaneous activity than was seen more dorsally.

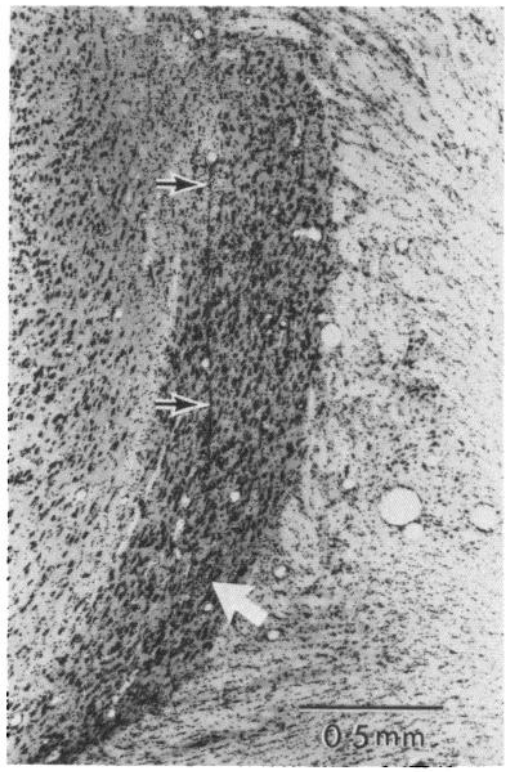

Figure 3. Electrode track (*small arrows*) and lesion (*large white arrow*) from *penetration 3* of Figure 2. The lesion marks the point where receptive fields reached the vertical meridian and visual responses ceased (see Fig. 2). At this coronal level, near the caudal pole, the visual area occupies all but a small ventral portion of the claustrum.

On 4 out of 18 penetrations in which fields reached the vertical meridian, they then progressed a short distance into the ipsilateral hemifield. The maximum excursion of receptive field centers was 10° (see Fig. 2, *penetration 1*).

The layout of the visual field in the mediolateral dimension is more complex and also differs at different anteroposterior levels. Figure 4 illustrates the results obtained in one cat in which six penetrations were made in a single coronal plane fairly far forward in the visual claustrum at the level marked *a* in Figure 1*F*. The penetrations were spaced at 0.5-mm intervals, and since the claustrum was 2.5 mm wide at this level, the outermost two penetrations (*1* and *6*) just grazed its medial and lateral edges. (Fig. 5 shows the tracks and marking lesions from this set of penetrations.)

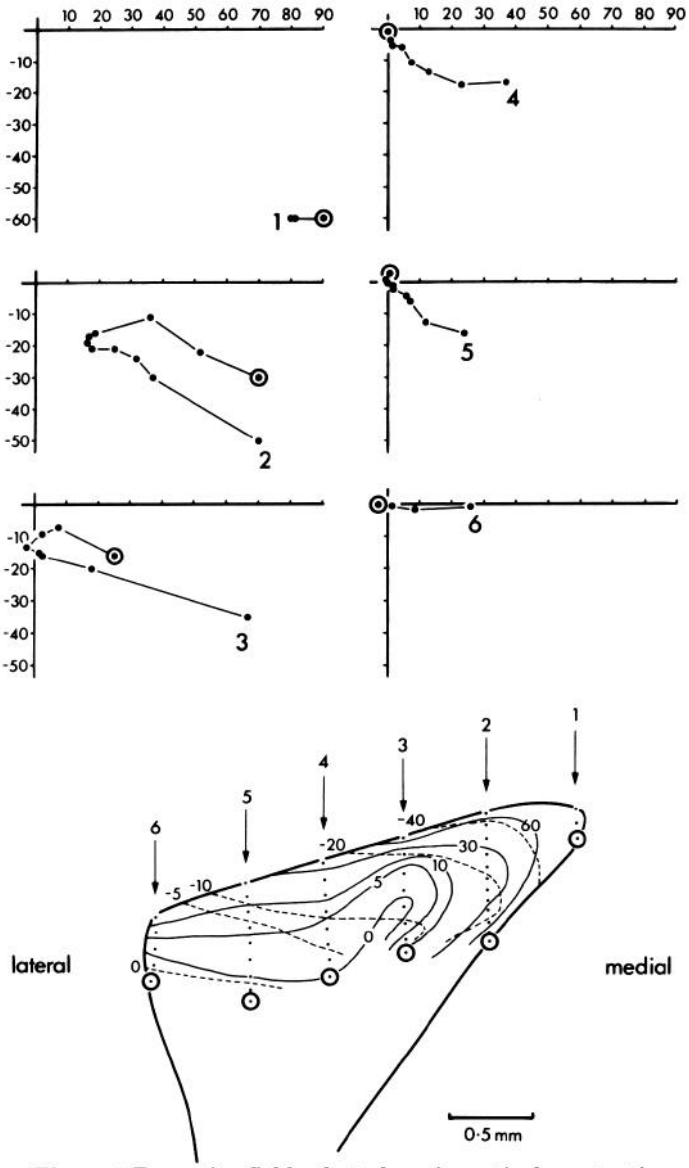

Figure 4. Receptive fields plotted on six vertical penetrations at different mediolateral positions in a single coronal plane toward the front of the left claustrum. Each penetration has been reconstructed on a separate field map (lower right quadrant only). Each receptive field is represented by a *dot* placed at its center. Each sequence begins at the *dot* indicated by the *penetration number* and ends with a lesion (*circled dot*) placed at the last visually responsive cell. The more medial penetrations begin with fields at relatively low elevations and peripheral azimuths, while laterally, the first recorded fields are higher and closer to the vertical meridian. Note especially the occurrence of reversals in the field progressions in *penetrations 2* and *3*. The *lower part* of the figure is a histological reconstruction of the tracks and lesions (see also Fig. 5), along with the isoazimuths (*solid lines*) and isoelevations (*dashed lines*) deduced from the recording data. The electrode tracks are shown as *trains of dots*, with each *dot* being the position (measured backward from the lesion) of a cell or group of cells whose receptive field is plotted in the appropriate map above.

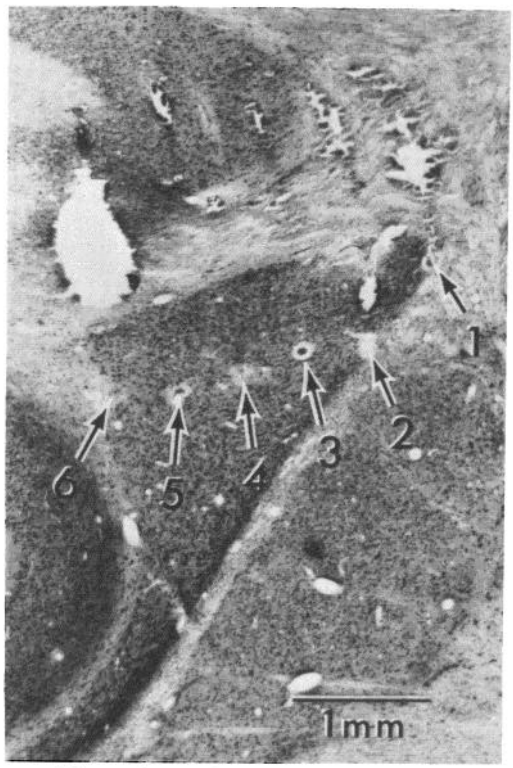

Figure 5. Electrode tracks and lesions (*1* to *6*) for the six penetrations illustrated in Figure 4. The lesions mark the last visually responsive units on each penetration and thus outline the lower border of the visual region. Note the broad, flat shape of the visual region at this anterior level (contrast with Fig. 3) and the large non-visual region beneath it.

The penetration closest to the middle of the claustrum, *4*, shows a progression of receptive fields similar to those described in Figure 2, namely a movement inward and upward across the lower contralateral quadrant. Visual responses ceased as receptive fields reached the representation of the vertical meridian. The more lateral penetrations (*5* and *6*) gave similar progressions except that the first fields encountered were not as far out in the visual field and the sequence of fields was slightly higher in the visual field than that of *penetration 4*.

The more medial penetrations (*3* and *2*) gave receptive field progressions that initially followed a similar trajectory. About halfway through these penetrations, however, the movement of receptive fields reversed, looping up and out and then downward as if to retrace in reverse the first part of the penetration. The rate of movement through the visual field was much slower in the neighborhood of the reversal than on other parts of the penetration. This can be seen from the close spacing of the *dots* in these regions of the reconstructed receptive field

trajectories of Figure 4: the *dots* represent equally spaced recording sites along each penetration.

Finally, the most medial penetration of the set (*1*) just grazed the dorsomedial corner of the claustrum. Receptive fields were far down in the extreme periphery and never moved inward.

The *lower part* of Figure 4 shows the layout of the isoazimuths and isoelevations in the coronal section just described. Laterally, the isoazimuths are reasonably flat, but medially, they sweep around in a sharp curve, following the dorsal outline of the nucleus. The reversals found on *penetrations 2* and *3* are caused by the curvature of the isoazimuths and not by the existence of a separate, mirror image representation of the visual field ventral to the first. The slowdown in the rate of movement through the visual field near the points of reversal was due to the fact that the electrode was traveling tangential to the curved isoazimuth lines at these points. The representation of the far periphery follows the claustral surface, starting about halfway across the nucleus, wrapping around the dorsomedial corner, and extending down the medial surface to the ventral limit of the visual claustrum. The representation of the vertical meridian, on the other hand, is flat laterally, but medially it is bundled up into a core that is enwrapped by the more peripheral azimuths. It does not reach the medial edge of the nucleus. Isoelevations are somewhat more simply arranged: they slant downward and medially, with the higher elevations represented laterally and the lower ones medially. Not all elevations are represented at this single coronal level; presumably, the upper field is represented more caudally and the extreme lower field more rostrally.

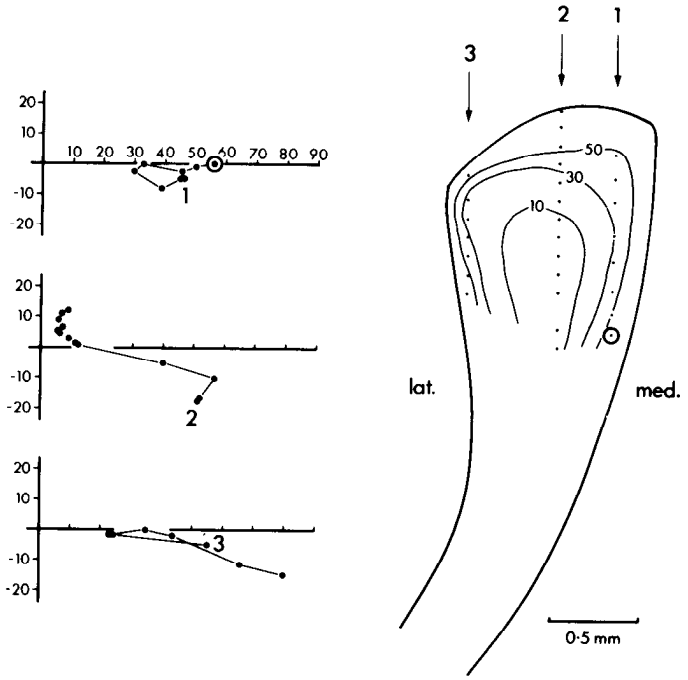

Figure 6. Receptive field progressions obtained on three electrode penetrations at a single coronal level, more posterior than that of Figure 4. Each penetration began with the receptive field indicated by an *arrow*. Only one of the three penetrations was terminated with a lesion (*1*, *circle*), but all three tracks were located histologically. The *diagram* on the *right* is the histological reconstruction, and it also shows the isoazimuth lines derived from the three penetrations (*solid lines*). The isoelevations are not shown; most of the receptive fields were close to the horizontal meridian. *lat.*, lateral; *med.*, medial.

TABLE I

List of experiments in which corticoclaustral projections were traced autoradiographically

The locations of the injection sites within the cortical visual field maps were determined by recording through the injection pipette except for the four cases marked by an asterisk, in which they were determined by examining the position of the resulting projection zone in the lateral geniculate nucleus within the known field map in that nucleus.

Cat	Cortical Area	Location in Visual Field		Tracer
		Azimuth	Elevation	
457	17	5°	7° down	[^{3}H]Proline
473	17	17°	2.5° down	[^{3}H]Proline
474*	17	0°	10° down	[^{14}C]Proline
474*	17	0°	2° up	[^{3}H]Proline
475	17	18°	1° down	[^{3}H]Proline
478	17	28°	4° down	[^{3}H]Proline
486*	17/18 border	0.5°	1° down	[^{3}H]Proline
493	17	0°	0°	[^{3}H]Proline
493	17	40°	0°	[^{3}H]Proline
526	17	14.5°	12.6° down	^{125}I-WGA
507	18	33°	0°	[^{3}H]Proline
525	18	5°	0.8° down	[^{3}H]Proline
491	19	1°	1° up	[^{3}H]Proline
522	19	28.5°	2.5° down	^{125}I-WGA
524	19	1°	3.5° down	^{125}I-WGA
536	21b	60°	10° up	[^{3}H]Proline
471*	PMLS[a]	30°	10° down	[^{3}H]Proline
509	PMLS	3° *ipsi*	0°	[^{3}H]Proline
527	PMLS	47°	13° down	^{125}I-WGA
477	PLLS[a]	23°	8° down	[^{3}H]Proline
543L	20a	19°	2° up	[^{3}H]Proline
543R	21a	9°	3° down	[^{3}H]Proline

[a] PMLS and PLLS refer to the posteromedial lateral suprasylvian and posterolateral lateral suprasylvian areas, respectively.

The caudal part of the visual claustrum is narrower and deeper than the rostral part, and hence, isoazimuths are curved more tightly. This is evident from the three penetrations illustrated in Figure 6 made at the level marked *d* in Figure 1*F*. The middle of the three penetrations reconstructed in Figure 6 (*2*) gave a typical sequence of receptive fields that moved rapidly from the far periphery toward the vertical meridian and upward. On both the medial and lateral penetrations (*1* and *3*), however, receptive fields progressed only a short distance inward before reversing direction and moving back toward the periphery.

The field map derived from these three penetrations is shown in Figure 6 (*right*). At this caudal level, both the medial and the lateral ends of the isoazimuth lines are curved strongly to match the narrow outline of the claustrum. The representation of the far periphery now not only occupies the dorsal and medial surfaces but also extends far down the lateral side, forming a horseshoe-shaped curve. The azimuths closer to the vertical meridian form a stack of successively smaller horseshoes, and the vertical meridian itself occupies a small core-like region at the ventral border of visual claustrum.

Observations made in all five cats studied in detail were consistent with the general outline of the claustral map as just described, and more fragmentary observations made in 12 other cats also agreed with this picture. There were minor variations that seemed to be related to slight differences in the overall shape and orientation of the nucleus. Thus, in some cats, the dorsal surface was more rounded, even at anterior levels, than is shown in Figure 1. In two cats, the claustrum was tilted so that its medial surface was vertical. These variations were doubtless caused by variations in the gyral pattern of the nearby cortex. They affected the exact layout of the map, but we never found evidence for discontinuous, jumbled, or multiple maps nor for any major rotation or inversion of the pattern described above.

Only one penetration was verified histologically as passing through the *claustrum parvum* (LeVay and Sherk, 1981). The single unit recorded in this diminutive structure had a very large receptive field but, in its other properties, was indistinguishable from units recorded in the main nucleus.

Anatomical mapping

General layout of the map. The autoradiographic results agreed closely with those obtained physiologically. In the first experiment of this series, we investigated the layout of the vertical meridian. Two injections were made on the border between areas 17 and 18 in one cat, one in the lower and the other in the upper visual field representation (see Table I). The lower field injection was of [^{14}C]proline, while the upper field injection was of [^{3}H]-proline. Two completely distinct zones of label resulted in the claustrum, one in front of the other. The anterior projection zone, a flattened ellipse of label, was shown by x-ray autoradiography to correspond to the [^{14}C]proline projection (Fig. 7*A*). The posterior zone was disk-shaped and represented the [^{3}H]proline projection (Fig. 7*B*). This and a number of other experiments (see Table I) indicate that the vertical meridian occupies a deep cylindrical zone, oriented rostrocaudally, that becomes flattened near its anterior limit, just as was found physiologically (see Fig. 1, *A* to *D*). Also in agreement with the physiological results, the lower visual field was situated rostrally and the upper field caudally. The peripheral field representation was investigated next in a second cat by making an injection in area 17 whose coordinates were 14° out and 1° down in the visual field. The resulting label in the claustrum formed an arch that enwrapped the vertical meridian representation on three sides (compare Fig. 7, *B* and *C*).

Figure 8 illustrates an experiment in which two injections were made on the horizontal meridian representation of area 17, one in the far periphery, 40° out (Fig. 8*A*) and the other at the area centralis (Fig. 8*B*). The peripheral injection labeled a rim of caudal claustrum that ran across the dorsal surface and wrapped far down both sides, while the central injection labeled a disk-like zone further ventral and anterior and located near the lateral

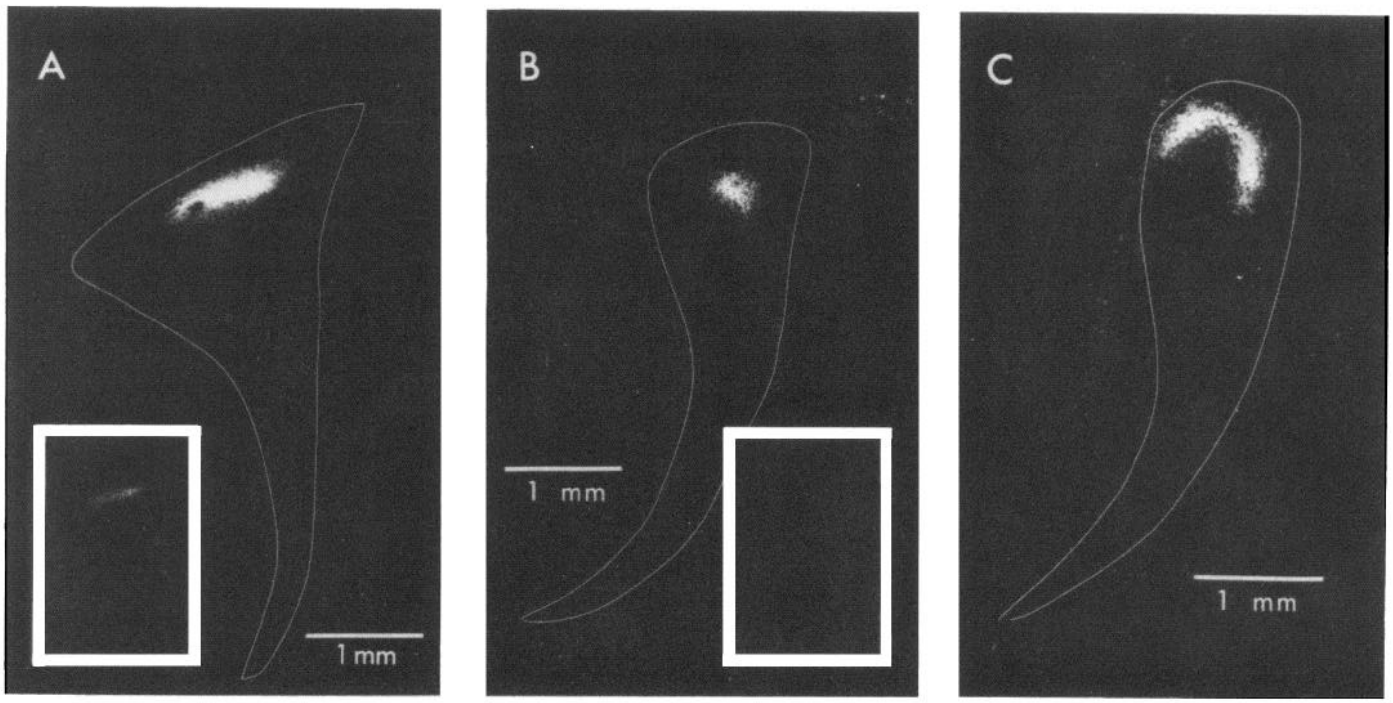

Figure 7. Autoradiographic label in the claustrum after injections of radioactive proline in area 17. *A* and *B* show the results of a double label experiment in one cat. *A*, [^{14}C]Proline was injected at a site on the vertical meridian and about 10° down and labeled a flattened ellipse near the anterior end of visual claustrum. The *inset* shows the same labeled zone on x-ray film, thus identifying it as being due to ^{14}C. The *inset* has been contrast-reversed so that silver grains appear *white*. *B*, [^{3}H]Proline was injected in the same cat but at a site about 2° above the area centralis, again on the vertical meridian. The labeled zone was shifted caudally in the claustrum, was disk-shaped rather than flattened, and failed to appear on x-ray film (*inset*). *C*, A second cat received a [^{3}H]proline injection that was more peripheral in area 17 (14° out and 1° below the horizontal meridian). The labeled zone formed a curved band that was shifted toward the surface of the claustrum.

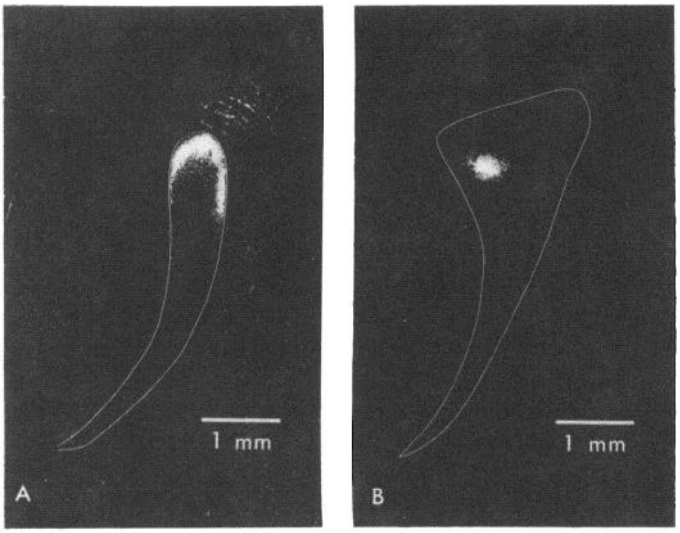

Figure 8. Labeled zones in the claustrum marking the horizontal meridian. *A*, One injection in area 17 was 40° out on the horizontal meridian, and the label appeared far caudally in the claustrum at its margin. *B*, In the same cat, an injection in the area centralis representation of area 17 labeled a round zone further rostral and deeper in the claustrum. Although both injections were of the same isotope ([^{3}H]proline), we are confident of these assignments from comparison with other autoradiographic experiments and with the results of physiological mapping.

border of the claustrum. These results indicate that the representation of the horizontal meridian in the claustrum occupies a plane that is tilted steeply back from the coronal plane. Again, this confirms our conclusions derived from physiological mapping.

As mentioned earlier, receptive fields of cells recorded at the ventral limit of the visual claustrum sometimes were centered up to 10° into the ipsilateral hemifield. We suspected that this representation might be generated by input from the lateral suprasylvian areas of the same hemisphere, and therefore, we made a [^{3}H]proline injection into area PMLS (Palmer et al., 1978) centered 3° out in the ipsilateral hemifield on the horizontal meridian. The resulting zone of labeling in the left claustrum (Fig. 9) was similar to that produced by injections of the cortical representation of the area centralis in other experiments. It may well have been centered slightly below this latter zone, as would be expected from the physiological results, but we could not be certain of this. This result is consistent with the idea that the ipsilateral field representation in the claustrum is derived from the ipsilateral lateral suprasylvian areas. It is also possible that contralateral visual areas make a contribution since a crossed corticoclaustral pathway has been demonstrated by Squatrito et al. (1980b), using massive injections of [^{3}H]proline. Our own cortical injections of [^{3}H]proline failed to label the contralateral claustrum, suggesting that the crossed projection is very weak.

The shape of the claustrum in cross-section at its caudal end is quite different from its shape further anterior. The consequences of this for the map can be seen by comparing the projections from two peripheral injection sites at different elevations in the visual field. Figure 10*A* shows the labeled zone following a [^{3}H]proline injection located 33° out and on the horizontal meridian in the right hemifield representation of area 18. (We will show below that the inputs from areas 17 and 18 to the claustrum are superimposed.) The shape of the labeled zone faithfully replicated the claustral outline, forming a long, arched band that extended far down both medial and lateral sides. In contrast, an injection of [^{3}H]proline centered 28° out and 4° down in the right hemifield representation of area 17 labeled a lopsided arc that followed the flat dorsal border of the claustrum and, turning its sharp medial corner, continued downward in a short, in-curving limb (Fig. 10*B*). Although this labeled band was quite long, it did not reach the dorsolateral corner of the claustrum and did not extend down the lateral surface.

These experiments confirmed that, away from the vertical meridian, single visual field points were represented as elongated, often curved zones in the claustrum. Their exact shape and orientation depended on their location within the overall map. A common feature of

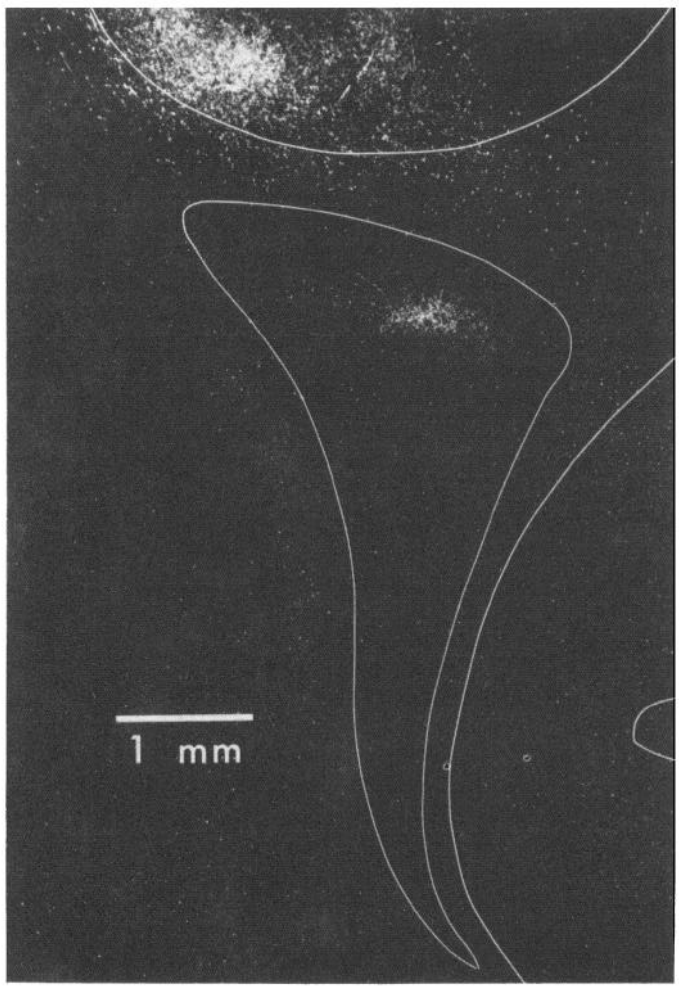

Figure 9. The projection zone resulting from an injection in the ipsilateral area PMLS at a site on the horizontal meridian and 3° out in the *ipsilateral* hemifield. The zone of label lay far rostral and at what is probably the ventral boundary of the visual region at this level. A projection to the overlying cortex is also visible.

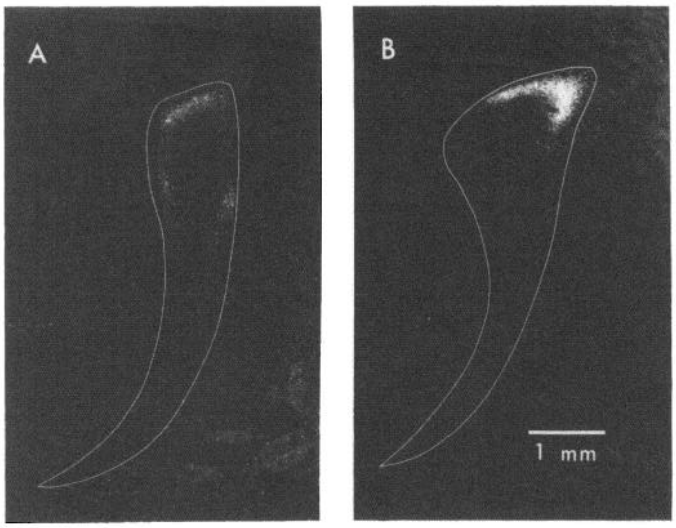

Figure 10. Projection zones in the claustrum resulting from two injections at different visual field elevations. *A*, An injection in area 18 33° out on the horizontal meridian labeled a symmetrical, elongated arch relatively far caudally. *B*, In another cat, an injection in area 17 located at a similar eccentricity (28°) but about 4° below the horizontal meridian labeled a region further anterior in the claustrum. The label took the form of an acutely angled band tilted into the dorsomedial corner of the nucleus.

these zones, not obvious from the single coronal sections illustrated, was that their lateral ends were shifted forward. This was consistent with the skewing of the isoelevation planes deduced physiologically (Fig. 1*E*).

Convergence of multiple cortical projections. We have described so far a single map in the visual claustrum that appears, within the resolution of our methods, to be orderly and without discontinuities or duplications. Since the visual claustrum receives inputs from at least five visual cortical areas, as described in the preceding paper (LeVay and Sherk, 1981), the question arises whether their projections to the claustrum are all superimposed. A plausible alternative would be that each projects to its own territory within the claustral map. Because of the redundancy in the physiologically determined map, in which a visual field point occupies a line, the map could be subdivided into discrete territories, with each one containing a complete hemifield representation and receiving input from a single area of visual cortex. We tested this possibility by making small injections of anterograde tracers at known retinotopic positions in areas 18, 19, and PMLS and comparing the labeled zones with those resulting from similar injections in area 17.

An injection in area 17 at a site 40° out on the horizontal meridian labeled a long rind of claustral surface near its caudal pole (Fig. 11*A*) as shown earlier, and an injection in area 18 at a site 33° out on the horizontal meridian resulted in a very similar region of label (Fig. 11*B*), although it was shifted slightly forward in the claustrum as one would predict for a point somewhat more central in the visual field. Moreover, injections on the vertical meridian, which thus involved both areas 17 and 18, invariably labeled only a single zone in the claustrum (Figs. 7, *A* and *B*, and 8*B*). Areas 17 and 18 thus appear to have co-extensive input territories. Area 19 was then injected; this time the site was close to the area centralis (1° out and 1° up), while a similar site (0° out and 2° up) was injected in area 17. The projection zones from areas 19 (Fig. 11*D*) and 17 (Fig. 11*C*) were both round and located deep in visual claustrum; again we would conclude that inputs from these two areas to the claustrum are completely overlapping. Finally, an injection of ^{125}I-WGA was made in area PMLS at a site with coordinates 47° out and 13° down. The most closely corresponding injection in area 17 was at a site 28° out and 4° down. The two projection zones had very similar shapes, each with a dorsal and medial limb meeting in an acute angle that mimicked the sharp dorsomedial corner of the claustrum (Fig. 11, *E* and *F*). The input from area PMLS occupied a zone dorsal and rostral to that from area 17, appropriate to its lower and more peripheral location in the visual field. Thus, although, in this case, the injection site coordinates did not match each other very closely, it is hard to escape the conclusion that the two labeled zones corresponded to neighboring isoprojection lines belonging to one map without any suggestion that either input was confined to its own domain. All other injections in these four cortical areas (see Table I) labeled isoprojection lines that fit the layout of the map described so far and thus support the conclusion that each area projects retinotopically to the entire claustral map.

We also made one injection in area 21a (Tusa and Palmer, 1980). The retinotopic coordinates of this site were 9° out and 3° down in the visual field. The resulting terminal labeling formed a thick, elongated band 0.5 mm below the dorsal surface of the claustrum at an anteroposterior level between *B* and *C* of Figure 1. The position of this labeled zone corresponded to that expected from the map described physiologically.

Discussion

The dorsocaudal claustrum was found to contain a single map of the visual field. Physiological and anatomical mapping yielded very similar descriptions of its organization: the contralateral half of the visual field is laid out in the claustrum with the upper fields located caudally, the lower ones rostrally, the far periphery at the claustral surface, and the vertical meridian at the lower limit of the visual region. There is but a single representation of the visual hemifield, and it is a unified map without discontinuities or duplications of one locus in noncontiguous parts of the claustrum.

Despite the relatively small size of the visual claustrum, the map that it contains appears to be quite orderly. It would be interesting to compare the receptive field scatter of cells lying along an isoprojection line with that found in area 17 (Hubel and Wiesel, 1962, 1965), since such scatter is a good measure of the degree of order in a map. However, we could not calculate this directly in the claustrum because the vertical electrode penetrations never ran along isoprojection lines. If, however, one examines the progressions of the receptive fields that were obtained from vertical electrode penetrations, it is striking that the receptive field centers described smooth trajectories through the visual field (e.g., Fig. 2), indicating a high degree of orderliness in the map.

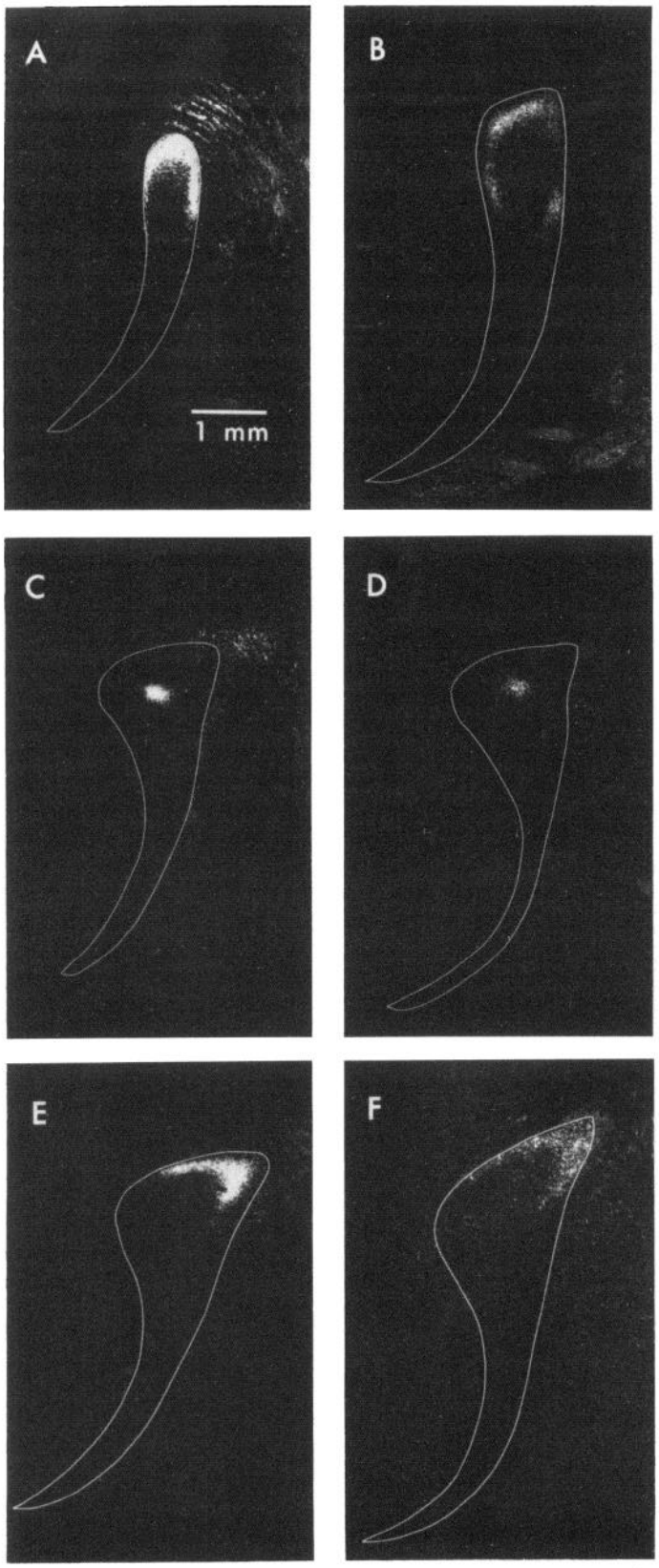

Figure 11. Labeled zones resulting from three injections in area 17 and three in other visual areas at similar visual field coordinates made in six cats. *A*, An injection 40° out on the horizontal meridian of area 17 labeled a rim of claustrum far caudally. *B*, In area 18, a somewhat more central injection, 33° out on the horizontal meridian, labeled a similar zone located slightly farther forward in the claustrum. *C*, In area 17, an injection on the vertical meridian and about 2° up labeled a round, fairly deep region. *D*, An injection in area 19 1° away from the vertical meridian and 1° up resulted in a virtually identical zone of label. *E*, In area 17, an injection fairly far peripheral (28° out) and about 4° down labeled a superficial, acutely angled zone. *F*, An injection of ^{125}I-WGA in area PMLS located still more peripherally (47° out and 13° down) resulted in a region of similar shape farther anterior in the claustrum. Both anterograde and retrograde transport contributed to this zone of label, and retrogradely labeled cells appear here as bright spots.

These trajectories contrast sharply with those obtained in vertical penetrations through the parabigeminal nucleus, for example, another small, unlaminated visual structure (Sherk, 1979). The claustral map is probably nearly as orderly as the map in area 17.

The absence of any lamination in the claustrum seems to have allowed its visual map to assume a layout quite different from those of the maps in laminated structures—visual cortex, lateral geniculate nucleus, or superior colliculus. As one would expect in any three-dimensional structure representing a two-dimensional field, a single line in the visual field, such as an isoazimuth or an isoelevation, is represented in the claustrum by a plane. What is remarkable about the claustral map is the organization of the isoazimuth planes. This is most straightforward in the posterior visual claustrum, where the space available is relatively narrow but deep. Here, the vertical meridian is represented as a cylindrical core at the ventral boundary of the visual region, running anteroposteriorly. A more peripheral azimuth occupies a sheet enwrapping this core on three sides, forming a long arch over it. A more distant azimuth, in turn, enwraps this arch and so on until the far periphery is reached, which is represented by the claustral surface and encloses the entire map medially, dorsally, and laterally.

Anteriorly, the visual claustrum is expanded considerably from side to side, but, as if in compensation, it becomes much shallower. Hence, the nature of the map also changes. The azimuths now form a stack of flat, approximately horizontal sheets, occupying most of the width of the nucleus, but, at the sharp dorsomedial corner, they are bent ventrally at an acute angle to continue for a short distance down the medial surface. The core representing the vertical meridian becomes flattened and expands laterally. The symmetrically wrapped map that is present caudally gradually rotates inward so that the dorsomedial corner of the claustrum becomes the apex of the stacked isoazimuth sheets. What caudally had been the lateral limb of an isoazimuth arch is now rotated dorsally and occupies most of the width of the claustrum, while the medial limb lies ventromedially and is severely truncated.

To some extent, the deformation of the visual field map observed in the claustrum may simply reflect the shape imposed on the nucleus by its packing between neighboring structures. The wrapped nature of the map, however, may function to expand the representation of the peripheral visual field. The central field is still favored compared to its actual area in the visual world, but,

compared to its representation in area 17, it appears to be significantly compressed. We would like to compare the magnification factors for the central field and the peripheral field in the claustrum with those in area 17 in order to verify this impression, but our data are not sufficiently detailed to calculate these values for the claustrum. Instead, we have asked what a visual field map in the claustrum would look like if it were constructed using the magnification factors operating in area 17. Such a hypothetical map, based on the values found by Tusa et al. (1978) for the horizontal meridian representation in area 17, is shown on the *left side* of Figure 12 and on the *right side* of this figure is the actual claustral map found physiologically at a level where the center of gaze is represented. In constructing the pseudo-map, we have proceeded as though isoelevation planes lie in the coronal plane, so that this section represents only horizontal meridian; in the claustrum, isoelevation planes are tilted about 45° backward, and thus the section of the real map in Figure 12 intersects the horizontal meridian only in the region of the area centralis. This does not affect, however, the validity of the comparison, which shows that, compared with area 17, the periphery of the visual field is considerably expanded in the claustrum, and the area centralis is compressed. A similar comparison with areas 18, 19, or PMLS would have yielded a still more striking difference, since these areas devote even less space to the periphery than does area 17 (Tusa et al., 1978; Palmer et al., 1978).

The distribution of labeled cells in the cortex after horseradish peroxidase injections in the claustrum (LeVay and Sherk, 1981) also suggested that this nucleus

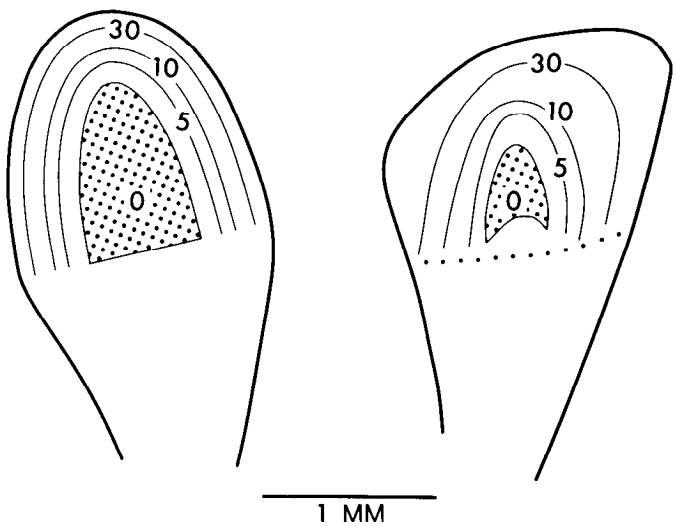

Figure 12. An imaginary map (*left*) of the visual field in the claustrum, constructed using the magnification factors found for area 17, contrasted with the actual claustral map (*right*) determined physiologically. The *shaded regions* in each case indicate the area centralis (0° to 2.5°), and the *lines* show isoazimuths. This comparison shows that the claustrum devotes relatively more space to the periphery and less to the area centralis than does area 17. The pseudo-map on the *left* represents only the horizontal meridian, while this is not true for the actual map on the *right*, since this section intersects the horizontal meridian only at the area centralis. A correction for this would increase the difference between the two maps further.

is particularly concerned with the peripheral visual field. The fraction of cells that projected to the claustrum was significantly greater in the part of area 17 devoted to peripheral visual field than in the representation of the central field. This nonuniform input may, in fact, provide the basis for the expanded representation of the periphery in the claustrum. Likewise, one might expect the return projection from claustrum to cortex to terminate most heavily in the representation of the periphery, and this did appear to be true in three out of four cases in which the claustrum was injected with [^{3}H]proline.

A question that is not strictly related to visual field mapping but that hinges on the density of cortical input to the claustrum is whether there are more cortical neurons that send axons to the nucleus than there are target cells to receive them. We can answer this tentatively if we make several assumptions and approximations. These are (*1*) that all cells in visual claustrum receive cortical innervation, which seems probable from our electron microscopic examination of degenerating corticoclaustral terminals (LeVay and Sherk, 1981); (*2*) that the fraction of cells in layer VI projecting to the claustrum is the same in different visual cortical areas, i.e., 3.5% in the representations of the peripheral visual field (more than 15° from the area centralis) and, on the average, half of this value in the central visual field (LeVay and Sherk, 1981); (*3*) that layer VI has the same cell density and average thickness in different cortical areas, taken to be 0.27 mm; and (*4*) that only five cortical areas project to visual claustrum (areas 17, 18, 19, 21a, and PMLS). From measurements of cell density in the claustrum and calculations of the volume of the visual area, we estimate the number of cells in the visual claustrum to be about 280,000. Relying on Tusa et al. (1978) and Tusa and Palmer (1980) for the approximate areas of the five cortical regions, we calculate that roughly 290,000 cells might project to the visual claustrum. (If we suppose that the six visual areas whose projections we have not investigated (the anteromedial lateral suprasylvian (AMLS), anterolateral lateral suprasylvian (ALLS), dorsal lateral suprasylvian (DLS), and ventral lateral suprasylvian (VLS) areas and areas 20b and 21b) also send afferents to the visual claustrum, the total number of afferents is increased only to 340,000. The small increase reflects the relatively small size of these areas.) This very approximate estimate suggests that the cortical afferents do not outnumber the claustral cell population greatly. A considerable degree of convergence may still occur, however, if the afferents branch extensively.

Two previous groups of investigators who studied the visual cortical projection to the claustrum (Jayaraman and Updyke, 1979; Squatrito et al., 1980a) concluded that it does not contain a visual field map. In contrast, Olson and Graybiel (1980) recently described the main axes of the visual map in the claustrum, and our results confirm and extend their findings. While Olson and Graybiel investigated the map electrophysiologically and autoradiographically, recording at those sites in the cortex where they injected amino acids, the earlier investigators used a more limited approach, injecting tracers into various cortical areas without recording cell activity. They relied instead on published maps to determine the

corresponding visual field locations and to decide what visual area was being injected. As the boundaries of different cortical areas and the exact layout of the map within each one are quite variable (Otsuka and Hassler, 1962; Tusa et al., 1978; Palmer et al., 1978), it is likely that this procedure obscured the retinotopic nature of the corticoclaustral projection.

From the autoradiographic experiments, we conclude that the projections from at least five visual cortical areas are superimposed retinotopically in the claustrum. Single claustral cells are therefore in a position to receive input from multiple visual cortical areas. Whether they actually do so remains unknown. Again, our conclusions differ from those of Jayaraman and Updyke (1979), who reported that areas 17 and 18 project to different regions in the nucleus. We think it possible that these different patterns were caused by their failure to inject retinotopically matching sites in the two areas.

Although it is quite common for single regions of the brain to receive a number of convergent and retinotopic visual projections, one generally finds at least a partial segregation of different inputs—for example, into different layers—as is seen in the geniculate and cortical inputs to area 17 or the retinal and cortical inputs to the superior colliculus. The intimate mixing of afferent projections seen in the claustrum does however have a parallel in the parvocellular C laminae of the lateral geniculate nucleus, which are reported to receive superimposed and retinotopic inputs from eight visual cortical maps (Raczkowski and Rosenquist, 1980). Unlike the claustrum, the C laminae also receive an input from two subcortical visual sources, the retina and the superior colliculus (Graybiel and Nauta, 1971). The absence of such afferents to the claustrum permits one to examine the response properties of a population of cells that are dependent solely on a convergent input from several visual cortical areas. This topic will be addressed in the following paper (Sherk and LeVay, 1981).

References

Carey, R. A., M. F. Bear, and I. T. Diamond (1980) The laminar organization of the reciprocal projections between the claustrum and striate cortex in the tree shrew, *Tupaia glis*. Brain Res. *184:* 193–198.

Graybiel, A. M., and W. J. H. Nauta (1971) Some projections of superior colliculus and visual cortex upon the posterior thalamus in the cat. Anat. Rec. *169:* 328.

Hubel, D. H., and T. N. Wiesel (1962) Receptive fields, binocular interaction and functional architecture in the cat's visual cortex. J. Physiol. (Lond.) *160:* 106–154.

Hubel, D. H., and T. N. Wiesel (1965) Receptive fields and functional architecture in two non-striate visual areas (18 and 19) of the cat. J. Neurophysiol. *28:* 229–289.

Jayaraman, A., and B. V. Updyke (1979) Organization of visual cortical projections to the claustrum in the cat. Brain Res. *178:* 107–115.

LeVay, S., and H. Sherk (1981) The visual claustrum of the cat. I. Structure and connections. J. Neurosci. *1:* 956–980.

Olson, C. R., and A. M. Graybiel (1980) Sensory maps in the claustrum of the cat. Nature *288:* 479–481.

Otsuka, R., and R. Hassler (1962) Ueber Aufbau und Gliederung der corticalen Sehsphäre bei der Katze. Arch. Psychiatr. Nervenkr. *203:* 212–234.

Palmer, L. A., A. C. Rosenquist, and R. J. Tusa (1978) The retinotopic organization of lateral suprasylvian visual areas in the cat. J. Comp. Neurol. *177:* 237–256.

Raczkowski, D., and A. C. Rosenquist (1980) Connections of the parvocellular C laminae of the dorsal lateral geniculate nucleus with the visual cortex of the cat. Brain Res. *199:* 447–451.

Sanderson, K. J. (1971) The projection of the visual field to the lateral geniculate and medial interlaminar nuclei in the cat. J. Comp. Neurol. *143:* 101–118.

Sherk, H. (1979) Connections and visual-field mapping in cat's tectoparabigeminal circuit. J. Neurophysiol. *42:* 1656–1668.

Sherk, H., and S. LeVay (1981) The visual claustrum of the cat. III. Receptive field properties. J. Neurosci. *1:* 993–1002.

Squatrito, S., P. P. Battaglini, C. Galletti, and E. Riva Sanseverino (1980a) Autoradiographic evidence for projections from cortical visual areas 17, 18, 19 and the Clare-Bishop area to the ipsilateral claustrum in the cat. Neurosci. Lett. *19:* 265–269.

Squatrito, S., P. P. Battaglini, C. Galletti, and E. Riva Sanseverino (1980b) Projections from the visual cortex to the contralateral claustrum of the cat revealed by an anterograde axonal method. Neurosci. Lett. *19:* 271–275.

Tusa, R. J., and L. A. Palmer (1980) Retinotopic organization of areas 20 and 21 in the cat. J. Comp. Neurol. *193:* 147–164.

Tusa, R. J., L. A. Palmer, and A. C. Rosenquist (1978) The retinotopic organization of area 17 (striate cortex) in the cat. J. Comp. Neurol. *177:* 213–236.